Advances in Analytical Chemistry 2015, 5(3A): 9-18
DOI: 10.5923/s.aac.201501.02

Electrooxidation of Urea on the Nickel Oxide Nanoparticles and Multi-walled Carbon Nanotubes Modified Screen Printed Electrode

Elaheh Lohrasbi, Mehdi Asgari*

NFCRS, NSTRI, Tehran, Iran

Abstract The multi-walled carbon nanotubes-NiO nanoparticles composite (MWCNT-NiO) prepare and the composite use for modification of screen printed electrode (SPE) for urea electrooxidation and impedimetric detection in alkaline medium (0.1 M NaOH). The nature and morphology of the MWCNT-NiO characterize by X-Ray Diffraction (XRD) and Transmission Electron Microscopy (TEM), respectively. The electrochemical behaviour of MWCNTs-NiO nanoparticles composite in an alkaline medium of urea study using cyclic voltammetry, chronoamperometry and Electrochemical Impedance Spectroscopy (EIS). The peak on the voltammogram for MWCNT-NiO composite modified electrode in alkaline medium of urea observes which is ascribed to the urea oxidation in alkaline medium. The obtained results discuss from the point of view of employment of the MWCNT–NiO composites for the catalytic electrodes of urea for hydrogen production.

Keywords Electrocatalysis, Nickel oxide, Nanoparticle, Carbon nanotube, Screen printed electrode, Urea, Electrooxidation

1. Introduction

The utilization of wastewater for useful fuel has been gathering recent attention due to society's need for alternative energy sources. The electrooxidation of urea found at high concentrations in wastewater simultaneously accomplishes fuel production and remediation of harmful nitrogen compounds that currently make their way into the atmosphere and groundwater [1]. Pure hydrogen was collected in the cathode compartment at 1.4 V cell potential, where water electrolysisdoes not occur appreciably. It was determined that aninexpensive nickel catalyst is the most active and stable for the process. The electrochemical treatment for urea-rich wastewater has recently become the focus of attention due to its potential applications, including wastewater remediation, hydrogen production, electrochemical sensors [2], and fuel cells [4, 5]. Various noble metal catalysts have been used for urea electro-oxidation [6-8].

Botte et al. [3] had successfully demonstrated the electrolysis of urea to produce hydrogen using Ni electrodes in alkaline medium. Some studies have been done in the past to identify the mechanism of urea hydrolysis in the presence of urease (with Ni active sites), both experimentally and theoretically [9, 10], according to the following reactions:

$$CO(NH_2)_{2\,(aq)} + 6OH^- \rightarrow N_{2(g)} + 5H_2O_{(l)} + CO_{2(g)} + 6e^- \quad (1)$$

$$Ni(OH)_{2(S)} + OH^- \rightarrow NiOOH_{(S)} + H_2O_{(l)} + e^- \quad (2)$$

$$6H_2O_{(l)} + 6e^- \rightarrow 3H_{2(g)} + 6OH^- \quad (3)$$

$$CO(NH_2)_{2\,(aq)} + H_2O_{(l)} \rightarrow N_{2(g)} + 3H_{2(g)} + CO_{2(g)} \quad (4)$$

But the research investigating the electrochemical oxidation mechanism of urea on nickel-based electrodes in alkaline medium is limited. Daramola et al. [9] studied the dissociation rates of urea in the presence of nickel oxyhydroxide (NiOOH) using density functional theory (DFT) methods and reported the desorption of CO_2 from urea as the rate-limiting step. They also reported that the NiOOH catalyst surface could be deactivated by the surface blockage due to CO groups. The nickel catalysts showed both higher current densities and lower oxidation potentials for the electro-oxidation of urea than those of the noble metal catalysts [2]. However, there is a potential gap between the theoretical electro-oxidation potential of urea (−0.46 V vs. SHE) and the observed oxidation potential using pure Ni catalysts (ca.0.45 V vs. SHE) [1, 11].

The existence of increased overpotential, and therefore high potential, for the oxidation of urea not only decreases the efficiency of the urea electrolysis process(see Eq. (4)), but also causes a certain degree of the oxygen evolution reaction (OER) in alkaline media [12]. The OER in alkaline media will lead to an extra energy loss for urea electrolysis

* Corresponding author:
mehdiasgari2002@yahoo.com (Mehdi Asgari)
Published online at http://journal.sapub.org/aac
Copyright © 2015 Scientific & Academic Publishing. All Rights Reserved

and make a negative impact on the stability of the nickel electrode. Therefore, the novel catalysts need to be synthesized to decrease the urea oxidation potential, promote urea electrolysis, and reduce the interference of the OER.

In the present work, the aim is concentrated on the electrocatalytic oxidation of urea in aqueous medium on screen printed modified electrode by NiO nanoparticles and MWCNTs. The catalysts were prepared by pulsed potential procedure on the multi-walled carbon nanotube. The nanoscale catalysts were characterized by TEM technique. Urea electrooxidation reaction was performed by means of electrochemical techniques such as cyclic voltammetry, chronoamperometry and electrochemical impedance spectroscopy. The performance of nanoscale catalysts was compared with that of corresponding single potential prepared catalysts to see whether nanocrystalline materials offer better properties for complete oxidation.

2. Experimental

2.1. Reagents and Apparatus

$NiSO_4.7H_2O$, boric acid, sodium hydroxide and urea of analytical reagent grade were prepared from Merck and were used without further purification.

The electrochemical experiments were carried out utilizing an Ivium Compactstate electrochemical analyzer equipped with a personal computer which was used for data storage and processing. A screen-printed carbon electrode (SPE) (3 mm in diameter) from Dropsens (Spain) was used as a planar three electrode based on a graphite working electrode, a carbon counter electrode and a silver reference electrode. The electrode was rinsed in deionized water and preconditioned in 0.1 M HCl solution by potential scanning in –400 to +1000mV at a scan rate of 100 mVs^{-1}.

For all experiments, 50µL of electrolyte was dropped on the SPE which all electrodes covered by electrolyte.EIS experiments carried out with a dc-offset potential of 750 mV and in the frequency range of 100000 to 0.01 Hz. Transmission electron microscopy (TEM) image was determined with a Philips CM10 TEM. A personal computer was used for data storage and processing.

2.2. Modified Electrode Preparation

Multi-walled carbon nanotubes (MWCNTs) were refluxed in the mixture of concentrated H2SO4:HNO3 (3:1) for 6 h to obtain the carboxylated multi-walled carbon nanotubes. The MWCNTs were washed with doubly distilled water and dried in vacuum at 80°C. MWCNTs (16 mg) and 5 µL of 5.0% nafion solution were dispersed in 5 mL water with ultrasonication for 1 h to get a homogenous suspension. 10 µL of the suspension was casted onto the surface of screen printed electrode and dried at room temperature.

The deposition baths were prepared using $NiSO_4.7H_2O$ with a total concentration of 40.0mM for all solutions. The pH of the bath was adjusted in 2 by adding boric acid. The pulse potential for producing NiO nanoparticles on the electrode was applied according toTable 1. The sizes of particles were controlled by changing the number of pulsesgone through in the depositions. It is clear that the increasing of the pulses caused the formation of a larger particle of modifier on the surface of SPE/MWCNT modified electrode. The prepared modified electrode was conditioned in 0.10 M NaOH solution by potential cycling between zero to 850 mV for about 30 cycles of potential scans with a scan rate of 100 mVs^{-1}. These parameters were obtained experimentally as optimum values for complete transformation of Ni (II) to Ni (III) and maximum activation of electrode surface in electrocatalytic oxidation of urea. All electrochemical investigations were performed at the room temperature.

Table 1. The used pulse potentials for preparation of NiO nanoparticles at the SPE /MWCNTs modified electrode

Level	Potential (V)	Duration (s)
1	-0.4	3
2	0	2.5
3	-0.4	3
4	0	2.5
5	-0.4	3
6	0	2.5
7	-0.4	3
8	0	2.5
9	-0.4	3
10	0	2.5

3. Result and Discussions

3.1. Nanostructure of the Nanocrystalline NiO-MWCNT Composite

In the TEM image of the nanocrystalline MWCNT-NiO composite shown in Fig.1a, it can be seen that the Nickel nanoparticles are distributed on the MWCNTs surface in the form of single stick. The Nickel oxide nanoparticles can therefore grow by repeated electrodeposition on the MWCNT matrix under a homogeneous distribution (Fig.1a). It can be deduced from these images that aggregation of the NiO nanoparticles is not obvious for all particles, and the nanoparticles are widely dispersed on the MWCNTs. Almost NiO particles are coated on MWCNT surface, and the particle sizes for all MWCNT samples are found to be constant 30–50 nm. The deposition of uniformly dispersed nanoparticles on MWCNTs is believed to be the result of uniform surface functional sites on all nanotubes that can be created in the chemical-wet oxidation of nitric acid. During the surface modification process, the surface oxides may act as active sites in adsorbing with Ni ions, thus forming an intermediate complex in the aqueous phase. Consequently, the surface coverage accessible to Ni (II) adsorption depends on the ionic concentration. Within the fixed period, the particles can grow in an equivalent size, in different particle densities over the surface of MWCNTs. It is well known that oxygen functional groups donate a surface polarity, i.e. surface electrostatic field, to carbon surfaces [13, 14]. The interaction of the electrostatic field on the surface with the dipole moment of water molecules plays a crucial role in determining the saturation of carbons in aqueous solutions.

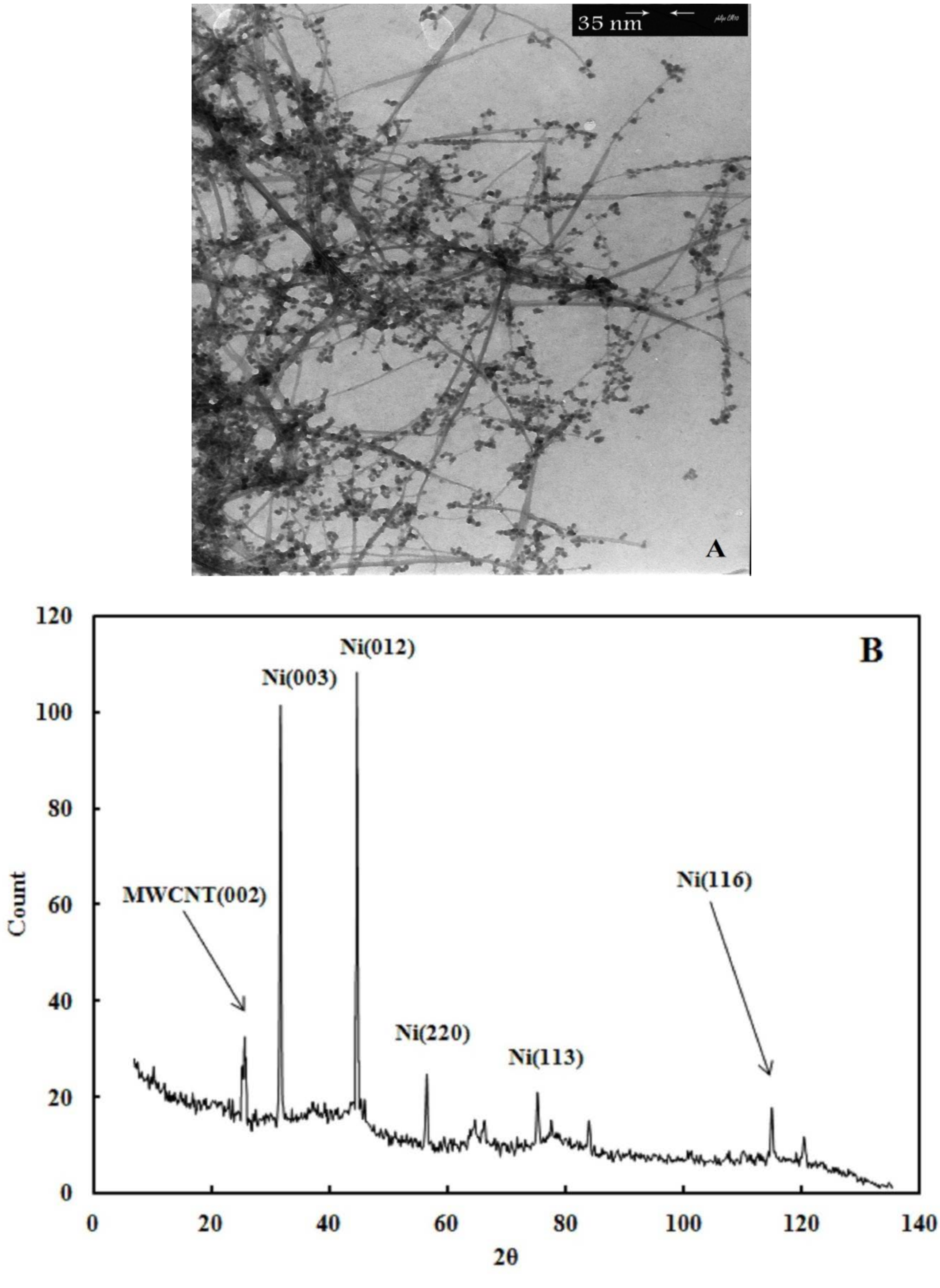

Figure 1. TEM image (A) and XRD pattern (B) of MWCNT/NiO composite

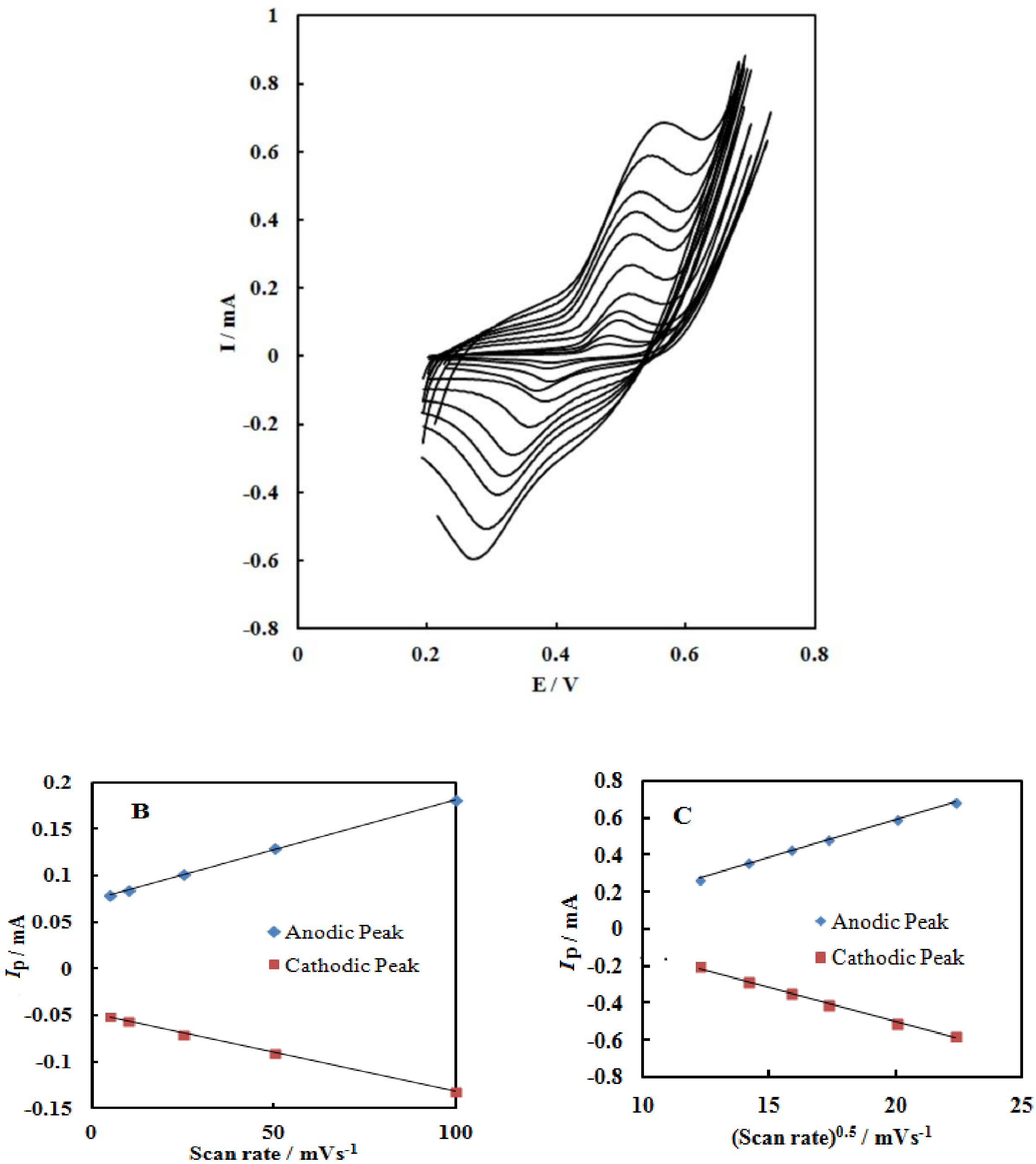

Figure 2. (A) cyclic voltammograms of the SPE/MWCNTs/NiO modified electrode in 0.10 M NaOH solution recorded at different potential scan rates in a wide range of 5-500 mVs^{-1}. (B)Variation of the anodic and cathodic peak currents versusthe potential scan rate values of 5-100mVs^{-1}. (C) Variation of the anodic and cathodic peak currents versusthe square root of potential scan rate values of 150-500mVs^{-1}

In order to further support the formation of MWCNTs -NiO composite, the X-Ray Diffraction (XRD) profile of the prepared nanocomposite was also represented, the result of which is shown in Fig. 1b. As seen, there is a typical reflection peak (002) for MWCNT at 21.8° in two curves [15]. The other diffraction peaks in NiO/MWCNT composite display the peaks of salt structured NiO, which can be assigned to (111), (200) and (220) (2θ) reflections of fcc phase NiO [16, 17], among which the two small diffraction peaks at 44° and 52° are matching Ni (111) and Ni (200) reflections, respectively [18].

3.2. Electrocatalytic Oxidation of Urea on the SPE/MWCNT-NiO Modified Electrode

Fig. 2A represents the cyclic voltammograms of the SPE/MWCNTs-NiO modified electrode in 0.10 M NaOH solution recorded at different potential scan rates in a wide range of 5-500mVs^{-1}. A pair of well defined peaks with peak potentials of 478mV and 385mV appears in the voltammograms for anodic and cathodic reactions, respectively, and the peak-to-peak potential separation (at the potential scan rate of 10mVs^{-1}) is 93mV. The voltammograms shown are similar to those previously reported [14, 16, 18], and the redox transition involved is attributed to the presence of Ni (II)/Ni (III) species. The peak-to-peak potential separation deviates from the theoretical value of zero and increases at higher potential scan rates. This result indicates a limitation in the charge-transfer kinetics, which is due to: (a) the chemical interactions between the electrolyte ions and the modifier film, (b) the dominance of electrostatic factors, (c) the lateral interactions of the redox couples present on the surface and/or (d) the non-equivalent sites present in the film.

The voltammograms shown in Fig. 2A also indicate that the anodic and cathodic peak currents are proportional to the potential scan rate at low values of 5-100mVs^{-1} (Fig. 2B). This result is attributable to the electrochemical activity of an immobilized redox couple on the surface. From the slope of this line and using [28]:

$$I_{\mathrm{p}} = (\frac{n^2F^2}{4RT})\upsilon A\Gamma^*$$

where Ip is the peak current, A is the electrode surface area and Γ^* is the surface coverage of the redox species and taking the average of both cathodic and anodic currents, a total surface coverage of the electrode with the modifier film of about 7.7×10^{-9}mol cm^{-2} is achieved. In the broad range of potential scan rates of 150-500mVs^{-1} (Fig. 2C), this dependency is of square root form, signifying the dominance of a diffusion process as the rate-limiting step in the total redox transition of the modifier film. This limiting-diffusion process, which is also reported for other Ni-based modified electrodes [19-21], may take place for the charge neutralization of the film during the oxidation/reduction reaction.

The modifier layer of MWCNTs-NiO on the electrode acts as a catalyst for the oxidation of urea in 0.10 M NaOH solution. Fig.3 shows the voltammograms recorded for this electrode in the absence (1) and in the presence of 0.10 M urea (2). An increase in the anodic peak current for peak (a) followed by the appearance of a new peak (b) with a more positive potential (with which these two peaks are overlapped in this figure) and disappearance of the cathodic peak(c) current during the reverse scan are the main effects observed upon the addition of urea to electrolyte. Obviously, the oxidation occurs in two regions of potential which overlap each other. The first region corresponds with the source from where Ni (Ш) species originates [19-23]. It is noted that the $Ni(OH)_2$/NiOOH transformation take place on the nickel electrode, quasi-reversibly. On the other hand, on SPE/MWCNTs-NiO modified electrode, this transformation occurs quasi-reversibly only to some extent and ultimately NiOOH is formed. With this potential, urea oxidation appears as an increase in $I_{\mathrm{p,a}}$ accompanied with disappearance in cathodic peak current in the reverse scan, which clearly shows that the applied modifier in this process participates directly in the electrocatalytic oxidation of urea. In the second region of potential, where only Ni (Ш) species exists on the electrode surface, a new anodic peak (b) with a powerful peak current with respect to that of the former one appears. The height of this peak increases linearly with urea concentration in the solution, showing that it concerns the process in which urea is involved. In the previous works [23-26], as regards the methanol electrooxidation, the authors concluded that the appearance of this new anodic peak (b) appeared due to methanol oxidation after the complete oxidation of Ni (П) to Ni (Ш), whereas, we inferred that urea could be adsorbed on Ni(III) when Ni(III)started to form on the electrode surface with the potential of 450 mV. The adsorbed urea oxidized during a chemical reaction in fast kinetics and produced Ni(II) and other products. In potential scans the newly produced Ni(II) oxidized to Ni(III) was materialized again and a new peak (b) appeared at the potential of 750 mV. This peak current depending on the urea concentration, increased in the urea concentration causing an increase in Ni(III) to Ni(II) transformation and then an increasing amount of the newly produced Ni(II) oxidized to Ni(III) emerged once more. The produced Ni(III) in these potentials oxidized the urea and in the switching potential, a large amount of Ni(III) was transformed to Ni(II), due to the decrease in this reaction cathodic peak. Accordingly, the catalytic role of Ni (Ш) for urea oxidation could be proposed as follows:

$$\text{Peak (a) } Ni(OH)_2 \leftrightarrow NiOOH + e^- + H^+ \quad (1)$$

$$NiOOH + Org \rightarrow Ni(OH)_2 + \text{Product} \quad (2)$$

$$\text{Peak (b) } Ni(OH)_2 \leftrightarrow NiOOH + e^- + H^+ \quad (3)$$

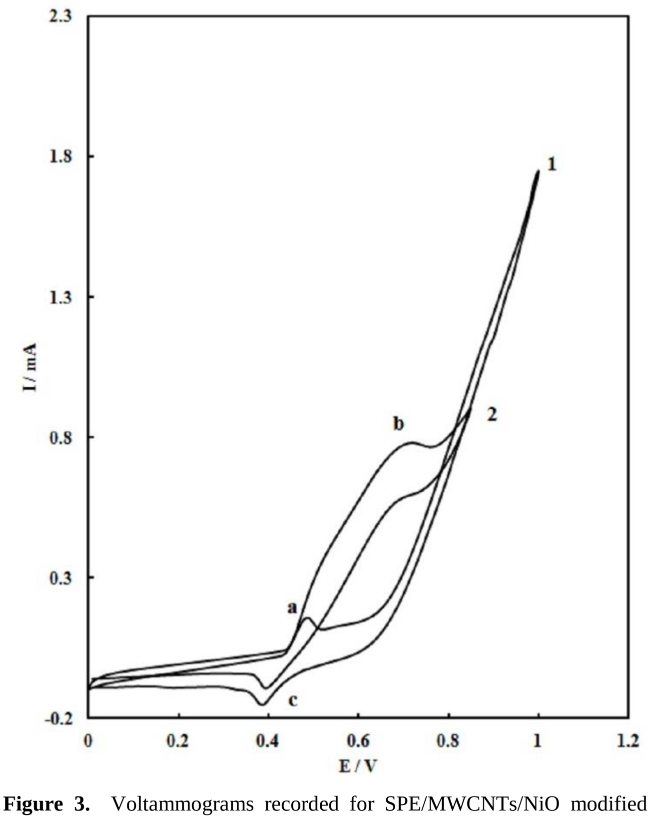

Figure 3. Voltammograms recorded for SPE/MWCNTs/NiO modified electrode in the absence (1) and in the presence of 0.10 M urea (2) with scan rate of 25 mVs^{-1}

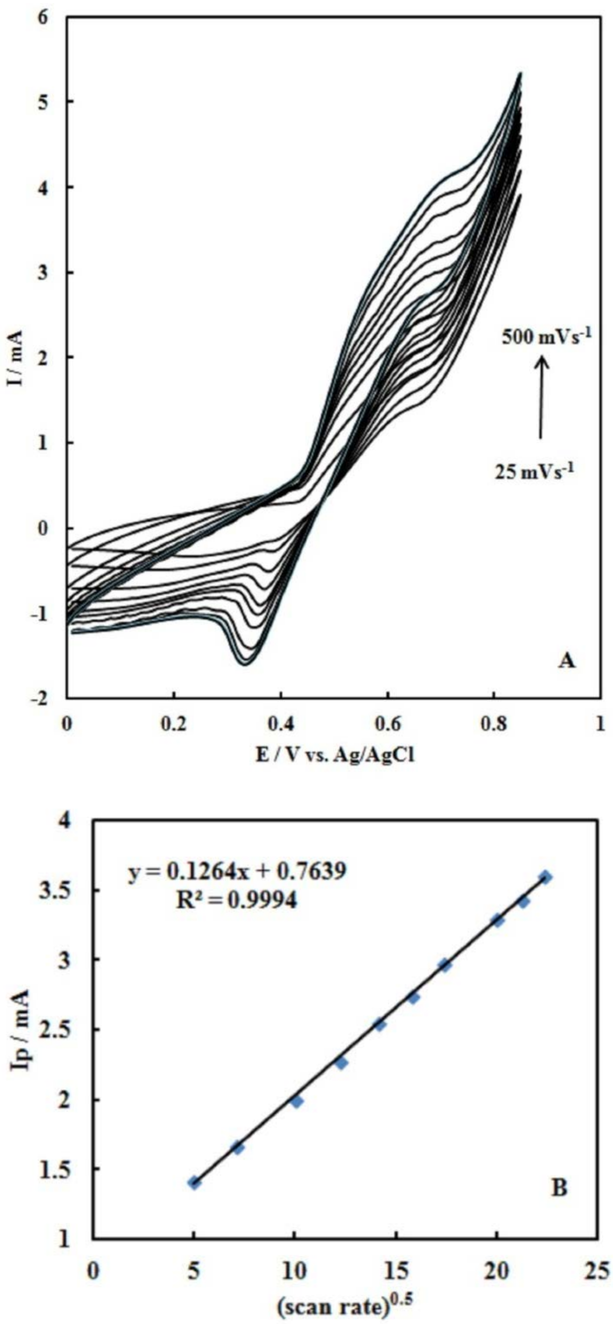

Figure 4. (A) The effect of scan rate on the peak current ratio at SPE/MWCNTs/NiO modified electrode in 0.10M NaOH + 0.10M urea. (B) Variation of the anodic peak currents versusthe square root of potential scan rate

The effect of the scan rate on the peak current ratio at SPE/MWCNTs-NiO modified electrode in 0.10M NaOH + 0.10M urea is shown in Fig. 4A. These voltammograms show that the anodic current for urea oxidation increases rapidly with increasing the potential scan rate. Indeed, the time window for urea oxidation process at the higher scan rates becomes very narrow avoiding the facile electron transfer between substrate and catalytic sites. However, the peak currents of the oxidation of $Ni(OH)_2$ and the reduction of NiOOH enhance with increasing the scan rate. Therefore, it can be concluded that the $Ni(OH)_2$/NiOOH transformation process is remarkably faster than the urea oxidation. Direct reaction between urea and NiOOH (formed on the electrode surface) produces NiO leading to a small increase in the anodic peak current.

Fig. 4B exhibits clearly that the anodic peak currents are linearly proportional to the square scan rate up to 500 mV s^{-1}. This figure shows that they are diffusion limited (Cottrell) [27].

Fig. 5 shows the effect of urea concentration on the anodic peak current at SPE/MWCNTs-NiO modified electrode in 0.10M NaOH. It is clearly observed that as the urea concentration increases, the peak height increases linearly with urea concentration up to 0.4 M. It can be assumed that the increase is due to the presence of a diffusion-controlled process that appears to play an important role at low urea concentrations. While the urea concentration exceeds this limit, the rate of the whole oxidation process seems to be limited by that of the catalytic process in origin and its rate depends on the reaction between urea and Ni(III) species, which is present in the film.

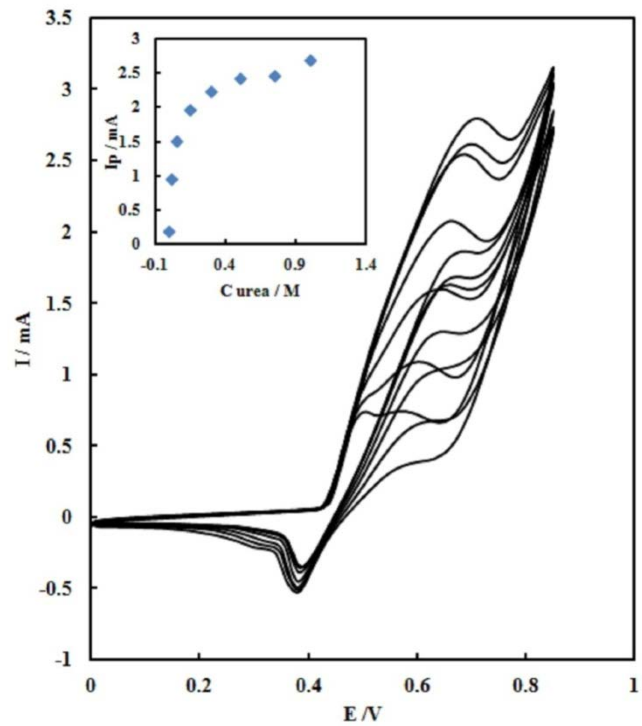

Figure 5. Cyclic voltammograms of the SPE/MWCNTs/NiO modified electrode in 0.10M NaOH containing different concentration of urea. Inset: Variation of the anodic peak currents versusthe urea concentration in the range of 0.003 to 1.0 M with scan rate of 25 mVs^{-1}

3.3. Chronoamperometric Study

The electrocatalytic oxidation of urea on the SPE/MWCNTs-NiO modified electrode was studied using chronoamperometry. Double-step chronoamperograms were recorded by setting the working electrode potentials to the desired values used to measure the catalytic rate constant on the modified surfaces. Fig. 6 shows the double-step chronoamperograms for the SPE/MWCNTs-NiO modified electrode in the absence and presence of different concentrations of urea. The applied potential steps were 750 and -200 mV. The current was negligible when the potential decreased to -200 mV, indicating that the electrocatalytic oxidation processes were irreversible.

The current observed from chronoamperograms was found to be in good agreement with the current observed from cyclic voltammetry. Also, the current increased as the urea concentration increased. This result supported our conclusion about the catalytic role of NiOOH for urea oxidation that started directly after the formation of the first amount of NiOOH on the electrode surface [23, 29].

In the inset of Fig. 6, plotting the net currents versus the minus square roots of time results has linear dependencies. Therefore, a diffusion-controlled process is dominant for electrooxidation of urea, as presented previously utilizing cyclic voltammetry (Fig.5). By means of the slopes of this line, the diffusion coefficients of the urea can be obtained according to the Cottrell equation [28]:

$$I = \frac{nFAD^{1/2}C}{(\pi t)^{1/2}} \quad (4)$$

where D is the diffusion coefficient, and C is the bulk concentration of urea. The mean value of the diffusion coefficient for urea is 2.48×10^{-5} cm^2s^{-1}.

According to the reported results, the described mechanism for the mediated oxidation of urea on the SPE/MWCNTs-NiO modified electrode surface can be approved and the corresponding kinetics is formulated as follows:

$$Ni(OH)_2 \underset{k_{-1}}{\overset{K_1}{\rightleftarrows}} NiOOH + H^+ + e^- \quad (5)$$

This reaction was followed by the oxidation of urea on the SPE/MWCNTs-NiO modified electrode via the reaction below:

$$NiOOH + urea \xrightarrow{K'} product + Ni(OH)_2 \quad (6)$$

In the preceding sequence of reactions, k_1 and k_{-1} are obviously potential dependent and their dependencies are as follows:

$$k_1 = k_1^0 \exp[\frac{\alpha nF(E-E^0)}{RT}] \quad (7)$$

$$k_{-1} = k_{-1}^0 \exp[\frac{(1-\alpha)nF(E-E^0)}{RT}] \quad (8)$$

where k_1^0 and k_{-1}^0 are the chemical rate constants measured at $(E\text{-}E^0)=0$ and α is the charge transfer coefficient. The rate laws for reactions 7 and 8 have the following forms:

$$v_1 = k_1\Gamma\theta_{II} - k_{-1}\Gamma\theta_{III} \quad (9)$$

$$v_2 = k_1\Gamma\theta_{III}C_{\text{urea}} \quad (10)$$

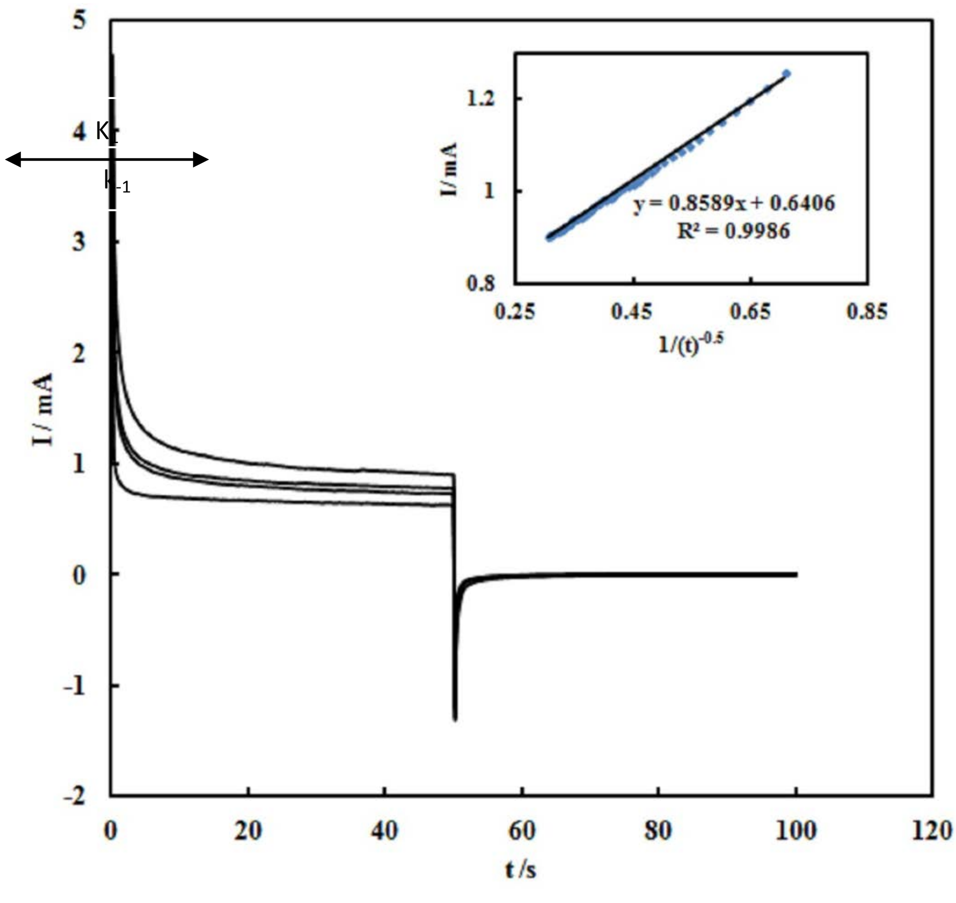

Figure 6. The double-step chronoamperograms for the SPE/MWCNTs/NiO modified electrode in the absence and presence of different concentrations of urea. The applied potential steps were 750 and -200 mV. Inset: plotting the net currents versus the minus square roots of time

where θs represent the fractional coverage of different nickel valence state, and C_{urea} is the bulk concentration of urea. The sum of nickel coverages is one for nickel and the rates of their coverage change are:

$$\frac{d\theta_{II}}{dt} = -\frac{d\theta_{III}}{dt} = -k_1\theta_{II} + k_{-1}\theta_{III} + k'\theta_{III}C_{urea} \quad (11)$$

Supposing that the steady-state approximations are dominating

$$\frac{d\theta_{II}}{dt} = -\frac{d\theta_{III}}{dt} = 0 \quad (12)$$

Therefore, the values of coverages are

$$\theta_{II} = \frac{k_{-1} + 2k' C_{urea}}{k_1 + k_{-1} + 2k' C_{urea}} \quad (13)$$

$$\theta_{III} = \frac{k_1}{k_1 + k_{-1} + 2k' C_{urea}} \quad (14)$$

Afterwards,

$$v_1 = \frac{2k'\Gamma C_{urea}}{k_1 + k_{-1} + 2k' C_{urea}} \quad (15)$$

Therefore, the faradic current will be calculated as

$$I_f = \frac{2FAk'\Gamma C_{urea}}{k_1 + k_{-1} + 2k' C_{urea}} \quad (16)$$

And the corresponding charge-transfer resistance is

$$R_{ct} = \left(\frac{dI_f}{dE}\right)^{-1} = \frac{(k_1 + k_{-1} + 2k' C_{urea})^2}{[2FAk'\Gamma C_{urea}\left(\frac{2\alpha Fk'\Gamma C_{urea}}{RT} + \frac{k_{-1}F}{RT}\right)]} \quad (17)$$

Eq. 17 is suitable for the calculation of the rate constants and the same equation can be used for validity test of the kinetics and mechanism. For this purpose, the electrochemical impedance spectroscopy was done.

3.4. Electrochemical Impedance Spectroscopy Study

Electrochemical impedance spectroscopy provides an effective method to probe the electron transfer resistance features of surface-modified electrodes. A typical shape of impedance spectrum (presented in the form of Nyquist plot) includes a semicircle region lying on the real part of complex impedance axis followed by a straight line. The semicircle part, observed at higher frequencies corresponds to the limited charge-transfer process, whereas the linear part of the spectrum is characteristic of the lower frequency range, and represents the diffusion-limited process. The semicircle diameter in the impedance spectrum equals to the charge-transfer resistance, R_{ct}. the experimental impedance spectra were fitted with computer-simulated spectra using an electronic circuit based on the Randles and Ershler theoretical model [30].

Fig. 7A shows the Nyquist diagrams of the SPE/MWCNTs-NiO modified electrode which were recorded at DC offset in 750 mV in both the absence and the presence of urea in 0.10M NaOH solution. In the absence of urea, a slightly depressed semicircle is observed, whereas in the presence of urea, a steady decrease in the diameter of the semicircle is noticed. The equivalent circuit compatible with these results is drawn in scheme 1.

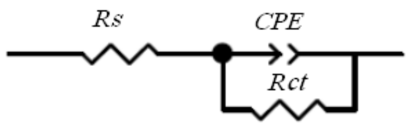

Scheme 1.

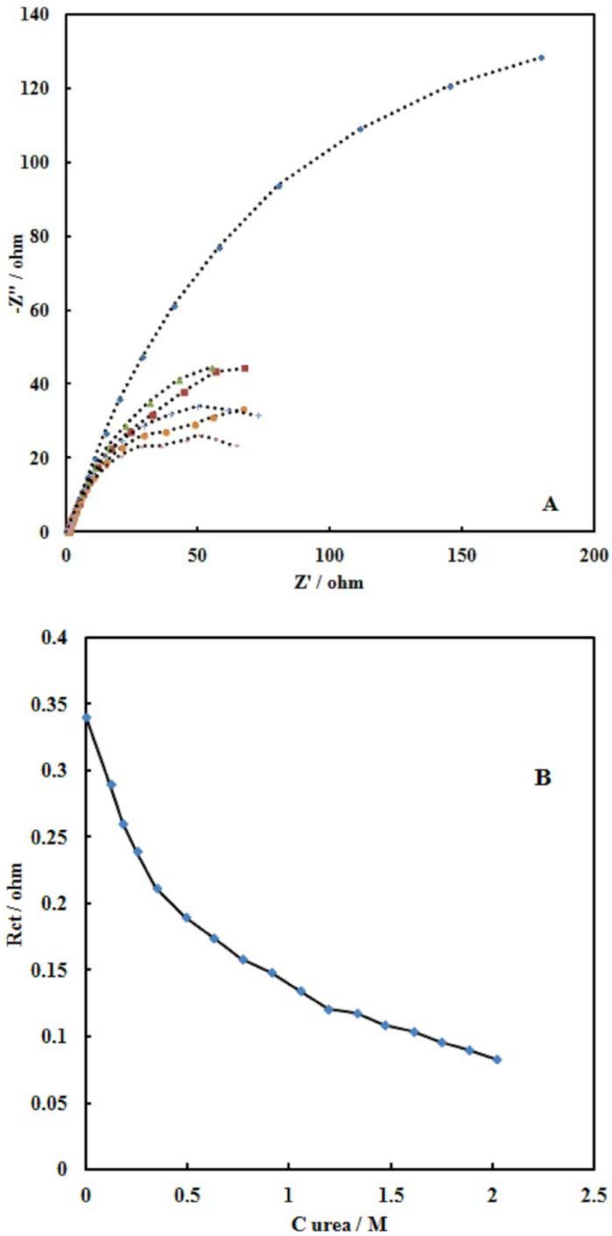

Figure 7. (A)Nyquist diagrams of a SPE/MWCNTs/NiO electrode recorded at 750 mV as the dc-offset for without and 0.001 to 0.6 M of urea. (B) Dependency of R_{ct} with urea concentration

In the presented equivalent circuit, R_s, *CPE* and R_{ct} represent the solution resistance, constant phase element and charge transfer resistance, respectively. The constant phase element corresponds to the double layer capacitance. To obtain a satisfactorily fitting Nyquist diagrams, it was necessary to replace the double layer capacitance with a constant phase element in the equivalent circuit. This replacement is because of microscopic roughness of the electrode surface, which causes an inhomogeneous distribution in the solution resistance and in the double layer capacitance [30]. The charge transfer resistance of the electrode reaction is the only circuit element which has a simple physical meaning which describes how fast the rate of charge transfer during electrocatalytic oxidation changes with the electrode potential or bulk concentration of urea in the solution. It should be noted that the diffusion process observed during the oxidation process using cyclic voltammetry and chronoamperometry probably would appeared at very low frequencies with a high time constant. This phenomenon did not appear in the scanning frequency range in the Nyquist diagram.

In contrast to cyclic voltammetry, EIS uses a small-amplitude perturbation signal, which makes it an excellent tool for obtaining highly resolved kinetic data related to thin films of electroactive surfaces [31, 32].

The chi-square goodness-of-fit, calculated for each fit by the FRA software employed, was systematically checked to validate all of the calculations performed [33]. For all cases studied in this work, the calculated values of chi-square for the mentioned equivalent circuit were in the range of 0.0001-0.01, much lower than the tabulated value for 5 degree of freedom (i.e., 67.505 at 95% confidence level), thus demonstrating a high significance of the final fit.

The dependency of the urea concentration on R_{ct} is presented in Fig.7B, where the initial sharp drops flatten out to very slow change by the increase in urea concentration. The results are further fitted in Eq. 17 to estimate the values of the rate constants. From the fitted equation and using the corresponding value of the previously calculated α, we worked out the mean values of the rate constants for nickel redox transition as $k_1^0 = 21.1$ and $k_{-1}^0 = 0.12$ $mol^{-1}s^{-1}$. The value of the obtained catalytic rate constant was $k' = 54.56$ $mol^{-1}s^{-1}$.

4. Conclusions

SPE/MWCNT-NiO modified electrode was checked for electro-oxidation of urea in alkaline medium. The electrode showed electrocatalytic oxidation for urea. Chronoamperometric works showed a powerful anodic current at the oxidation potential of low-valence nickel hydroxide in further support of the mediated electro-oxidation. A kinetic model was developed and the kinetic parameters were calculated using the urea concentration dependency of charge transfer resistance derived from the impedance studies. Using cyclic voltammetry and chronoamperometry techniques, the kinetic parameters of urea, such as charge-transfer coefficient and diffusion coefficient for oxidation, were determined.

ACKNOWLEDGEMENTS

The support of this work by research grants from the NSTRI Research Council is gratefully acknowledged.

REFERENCES

[1] B.K. Boggs, R.L. King, G.G. Botte, Chem. Commun. 32 (2009) 4859- 61.

[2] Ch-M. Yang, I-Sh. Wang, Yi-T. Lin, Ch-H. Huang, Tseng-Fu.Lu, Ch-En. Lue, D. G.Pijanowska, Mu-Yi.Hua, Chao-S. Lai, Sensors and Actuators B Chem 187(2013) 274-279.

[3] G. G. Botte (2009) US Patent Application No. 0095636 A1.

[4] D. Das, T.N. Veziroglu, International Journal of Hydrogen Energy 26 (2001) 13-28.

[5] R.L. King, G.G. Botte, Journal of Power Sources 196 (2011) 2773-2778.

[6] V.A. Gromyko, T.B. Tsygankova, V.B. Gaidadymov, Y.B. Vasil'ev, V.S. Bagotskii, Elektrokhimiya 10 (1974) 57-61.

[7] G. Horanyi, G. Inzelt, E.M. Rizmayer, J. Electroanal. Chem. Interfacial Electrochem. 98 (1979) 105-117.

[8] W. Simka, J. Piotrowski, G. Nawrat, Electrochim. Acta 52 (2007) 5696- 5703.

[9] D.A. Daramola, D. Singh, G.G. Botte, J. Phys. Chem. A 114 (2010) 11513-11521.

[10] R.L. King, G.G. Botte, J. Power Sources 196 (2011) 9579-9584.

[11] R.L. King, G.G. Botte, J. Power Sources 196 (2011) 2773-78.

[12] M. Vidotti, M.R. Silva, R.P. Salvador, S.I. Cordoba de Torresi, L.H. Dall'Antonia, Electrochim. Acta 53 (2008) 4030-34.

[13] K. Kinoshita, Carbon: electrochemical and physicochemical properties. New York: John & Wiley; 1987.

[14] C. T. Hsieh, H.Teng, Carbon 40(2002) 667-674.

[15] D. J. Guo, H. L. Li, Carbon 43(2005)1259-1264.

[16] F. B. Zhang, Y. K. Zhou, H. L. Li, Mater. Chem. Phys. 83 (2004) 260- 264.

[17] X. M. Liu, X. G. Zhang, Electrochim. Acta 49(2004)229-232.

[18] C. C. Hu, C. Y. Lin, T. C. Wen, Mater. Chem. Phys. 44(1996) 233-238.

[19] M. Asgari, M. Ghannadi Maragheh, R. Davarkhah, E. Lohrasbi, J. The Electrochem. Soc. 158 (12) (2011) K225-k229.

[20] A. N. Golikand, M. Asgari, M. Ghannadi Maragheh, S. Shahrokhian, J. Electroanal. Chem. 588(2006)155-160.

[21] A. N. Golikand, S. Shahrokhian, M. Asgari, M. Ghannadi Maragheh, L. Irannejad, A. Khanchi, J. Power Sources 144(2005)21-27.

[22] A. Seghiour, J. Chevalet, A. Barhoum, F. Lantelme, J. Electroanal. Chem. 442 (1998) 113-123.

[23] A.A. El-Shafei, J. Electroanal. Chem. 471 (1999) 89-95.

[24] G. Ve´rtes, G. Hora´ny, J. Electroanal. Chem. 52 (1974) 47-53.

[25] P.M. Robertson, J. Electroanal. Chem. 111 (1980) 97-104.

[26] J. Taraszewska, G. Rostonek, J. Electroanal. Chem. 364 (1994) 209-213.

[27] J.A. Harrison, Z.A. Khan, J. Electroanal. Chem. 28 (1970) 131-138.

[28] A.J. Bard, L.R. Faulkner, Electrochemical Methods, Wiley, New York, 2001.

[29] R. M. A. Tehrani, S. Ab Ghani, Fuel Cells 9(2009)579- 587.

[30] A. Maritan, F. Toigo, Electrochim. Acta 35 (1990) 141- 145.

[31] M.D. Levi, D. Aurbach, J. Electrochem. Soc. 14 9(2002) E215-E221.

[32] J. R. McDonald, Impedance Spectroscopy, Wiley, New York, 1987.

[33] R.K. Shervadani, A. Mehrjardi, N. Zamiri, Bioelctrochem. 69 (2006) 201-208.